

PAPER • OPEN ACCESS

Traceable reference dosimetry in MRI guided radiotherapy using alanine: calibration and magnetic field correction factors of ionisation chambers

To cite this article: Ilias Billas et al 2021 Phys. Med. Biol. 66 165006

View the article online for updates and enhancements.

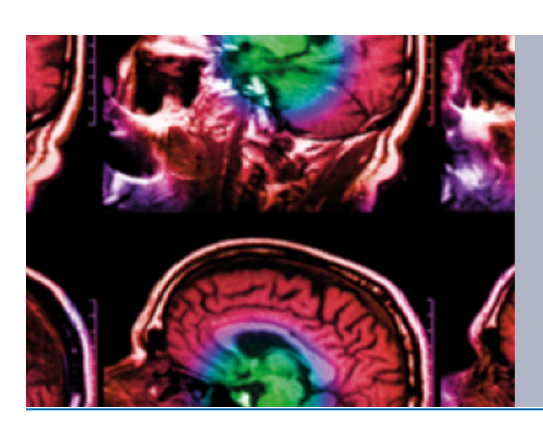
You may also like

- Performance Simulation of Tubular Segmented-in-Series SOFC Using Simplified Equivalent Circuit Shun Yoshida, Tadashi Tanaka and Yoshitaka Inui
- An Atmospheric Correction Algorithm For GF-2 Image Based On Radiative Transfer Model

Hongye Cao, Ling Han, Tianqi Zhang et al.

 Experimental determination of magnetic field correction factors for ionization chambers in parallel and perpendicular orientations

Stefan Pojtinger, Marcel Nachbar, Sarah Ghandour et al.



IPEM IOP

Series in Physics and Engineering in Medicine and Biology

Your publishing choice in medical physics, biomedical engineering and related subjects.

Start exploring the collection-download the first chapter of every title for free.

Physics in Medicine & Biology





OPEN ACCESS

RECEIVED

5 October 2020

REVISED

12 May 2021

ACCEPTED FOR PUBLICATION 28 May 2021

PURIISHED

6 August 2021

Original content from this work may be used under the terms of the Creative Commons Attribution 4.0 licence

Any further distribution of this work must maintain attribution to the author(s) and the title of the work, journal citation and DOI.



PAPER

Traceable reference dosimetry in MRI guided radiotherapy using alanine: calibration and magnetic field correction factors of ionisation chambers

Ilias Billas^{1,2,*}, Hugo Bouchard³, Uwe Oelfke² and Simon Duane¹

- ¹ National Physical Laboratory, Teddington, United Kingdom
- ² Joint Department of Physics, The Institute of Cancer Research and The Royal Marsden NHS Foundation Trust, London, United Kingdom
- ³ Université de Montréal, Département de Physique, Montréal, Canada and Centre Hospitalier de l'Université de Montréal, Montréal, Canada and Centre de recherche du CHUM, Montréal, Canada
- * Author to whom any correspondence should be addressed.

E-mail: ilias.billas@npl.co.uk

Keywords: MRI-linac, magnetic field, traceable reference dosimetry, magnetic field correction factors, alanine dosimetry

Abstract

Magnetic resonance imaging (MRI)-guided radiotherapy (RT) (MRIgRT) falls outside the scope of existing high energy photon therapy dosimetry protocols, because those protocols do not consider the effects of the magnetic field on detector response and on absorbed dose to water. The aim of this study is to evaluate and demonstrate the traceable measurement of absorbed dose in MRIgRT systems using alanine, made possible by the characterisation of alanine sensitivity to magnetic fields reported previously by Billas et al (2020 Phys. Med. Biol. 65 115001), in a way which is compatible with existing standards and calibrations available for conventional RT. In this study, alanine is used to transfer absorbed dose to water to MRIgRT systems from a conventional linac. This offers an alternative route for the traceable measurement of absorbed dose to water, one which is independent of the transfer using ionisation chambers. The alanine dosimetry is analysed in combination with measurements with several Farmer-type chambers, PTW 30013 and IBA FC65-G, at six different centres and two different MRIgRT systems (Elekta Unity™ and ViewRay MRIdian™). The results are analysed in terms of the magnetic field correction factors, and in terms of the absorbed dose calibration coefficients for the chambers, determined at each centre. This approach to reference dosimetry in MRIgRT produces good consistency in the results, across the centres visited, at the level of 0.4% (standard deviation). Farmer-type ionisation chamber magnetic field correction factors were determined directly, by comparing calibrations in some MRIgRT systems with and without the magnetic field ramped up, and indirectly, by comparing calibrations in all the MRIgRT systems with calibrations in a conventional linac. Calibration coefficients in the MRIgRT systems were obtained with a standard uncertainty of 1.1% (Elekta Unity™) and 0.9% (ViewRay MRIdian™), for three different chamber orientations with respect to the magnetic field. The values obtained for the magnetic field correction factor in this investigation are consistent with those presented in the summary by de Pooter et al (2021 Phys. Med. Biol. 66 05TR02), and would tend to support the adoption of a magnetic field correction factor which depends on the chamber type, PTW 30013 or IBA FC65-G.

1. Introduction

Recently, magnetic resonance imaging (MRI)-guided radiotherapy (RT) (MRIgRT) was introduced in the community and the clinical proof-of-principle was delivered (Acharya et al 2016, Fischer-Valuck et al 2017, Raaymakers et al 2017). This highly advanced technique consists of using a new machine integrating a conventional linear accelerator (linac) with an MRI scanner, this way enabling real-time imaging during radiation treatment without additional radiation dose from the imaging system. This entirely new approach to

RT promises personalised adaptive planning using the advantage of MRI to produce high-contrast dynamic images and advanced optimisation techniques to adapt treatment delivery to the moving anatomy.

A known effect, and one investigated extensively in the literature, is the influence of the constant magnetic field of the MRI scanner on radiation dosimetry. This field alters the direction of motion of charged particles, due to the Lorentz force, and consequently will affect the detector response and the dose to medium. Several studies have investigated the influence of the magnetic field on different detectors, such as: ionisation chambers (Reynolds *et al* 2013, O'Brien *et al* 2016, Spindeldreier *et al* 2017, Pojtinger *et al* 2018, Cervantes *et al* 2020), Gafchromic film (Delfs *et al* 2018, Billas *et al* 2019), alanine (Billas *et al* 2020), Fricke dosimeters (Trachsel *et al* 2020) and Presage (Costa *et al* 2018). Other studies have quantified the effect of the magnetic field on the absorbed dose to water (Raaymakers *et al* 2004, O'Brien *et al* 2016, Billas *et al* 2020).

At the current stage, the scope of existing high energy photon therapy dosimetry protocols, i.e. Lillicrap $et\ al$ (1990) and Eaton $et\ al$ (2020), Almond $et\ al$ (1999), Andreo $et\ al$ (2000), Palmans $et\ al$ (2017), etc, does not include dosimetry in MRIgRT. Although some reference conditions (i.e. source-to-detector distance, depth in water, field size, etc) for the realisation of the absorbed dose may be achieved in MRIgRT, the effects of the magnetic field on dosimetry are not considered, making these protocols invalid (unless and until those effects can be shown to be negligible).

In achieving traceable dosimetry for MRIgRT, a choice must be made between:

- (i) realising absorbed dose to water directly, in a beam, in the magnetic field (using a primary standard), and
- (ii) transferring absorbed dose to water to the beam in a magnetic field (using a transfer standard), from a realisation in a beam in zero magnetic field.

In both options the user's chamber is calibrated in the user's beam, in the presence of the magnetic field. Either way, there is no need for a magnetic field correction factor for the user's chamber. However both options require an adequate understanding of how detector response may be affected by the magnetic field, whether that detector is (i) the primary standard, whose correction factors may be magnetic field dependent, or (ii) the transfer standard, whose absorbed dose sensitivity may be magnetic field dependent. There is a third choice, if a magnetic field correction factor is available for the user's chamber, in which:

(i) absorbed dose is realised, and the user's chamber is calibrated, in a beam with no magnetic field.

Subsequent measurements in the MRIgRT system with the user's chamber are then traceable, even in option (iii) provided its magnetic field correction factor is valid.

The realisation of the physical quantity absorbed dose to water is achieved by a primary standard, which makes an absolute measurement, based on the definition of the quantity, and which is tied into the metrology infrastructure of international comparisons of equivalent standards.

Two primary standard laboratories, VSL (Van Swinden Laboratory, which is the Dutch Metrology Institute) and PTB (Physikalisch-Technische Bundesanstalt, which is the German Metrology Institute), and a work from D'Souza *et al* (2020) have performed a direct and fundamental measurements of the absorbed dose to water in an MRI-linac with water calorimeters (de Prez *et al* 2016, 2019a, D'Souza *et al* 2020, Krauss *et al* 2020). Without the need for the magnetic field correction factor, these dosimeters can directly calibrate ionisation chambers in an MRI-linac.

Several studies suggested a formalism (O'Brien et al 2016, van Asselen et al 2018, Malkov and Rogers 2019, Cervantes et al 2020) that can be used for the determination of the absorbed dose to water. This formalism introduces a magnetic field strength-dependent correction factor to modify the detector calibration coefficient from zero magnetic field. Data sets of correction factors are accessible from published studies, which may be integrated into existing conventional protocols for the improvement of the dosimetry in MRIgRT. Nevertheless, as pointed out in a recent review paper (de Pooter et al 2021), the performance of ionisation chambers in magnetic fields is still yet to be fully understood. It has become clear that the magnetic field enhances the sensitivity of ionisation chamber response to some aspects of design that in conventional conditions were less important. The presence of small air gaps (Hackett et al 2016, Agnew et al 2017), the dead volume (Malkov and Rogers 2017, Pojtinger et al 2019, Cervantes et al 2020), manufacturing tolerances (Cervantes et al 2020) and intra-type variability, especially in small cavity chambers, all tend to increase the uncertainty of ionisation chamber-based dose measurements. Although values for the magnetic field correction factor have been published for various ionisation chamber types, there remains a need for more data and a better understanding, of all of these effects. As mentioned in de Pooter et al (2021), early publications on dosimetry in magnetic fields have some *flaws*, as the importance of some potential effects was not yet appreciated. Correction factors from such studies must be carefully assessed before combining them with values determined more recently.

This study aims to demonstrate the validity of using alanine as the transfer standard in the second option, identified above as (ii), and to provide further data for the magnetic field correction factor, to support the third option (iii), to achieve traceability in dosimetry for MRIgRT systems which is compatible with the existing standards and calibrations available for conventional RT. These options are the only way to avoid a requirement for the widespread use of primary standards directly in users' MRIgRT systems. Alanine dosimetry has only a modest sensitivity to the presence of a magnetic field at the time of irradiation, and the magnetic field dependence is less strong than for reference class ionisation chambers. The alanine was calibrated at NPL (National Physical Laboratory, which is the United Kingdom Metrology Institute) in a ⁶⁰Co beam at zero magnetic field and its calibration coefficient converted to conventional linac by the application of a beam quality correction factor. Its absorbed dose response is corrected for the effect of the magnetic field based on previous work (Billas *et al* 2020) which characterised the behaviour of, and described the advantages of, using alanine for MRIgRT dosimetry.

I Billas et al

The investigations reported here were carried out in the currently commercial MRIgRT systems, i.e. Elekta Unity™ (Elekta Instrument AB Stockholm, Sweden) and ViewRay MRIdian™ (ViewRay Inc., Oakwood, USA). Comprehensive measurements for the determination of the absorbed dose to water in a magnetic field, including the investigation of the influence quantities on the detector signal, were performed. The alanine magnetic field correction factors, for the Elekta Unity™ and the ViewRay MRIdian™ beam qualities, were obtained, and the effect of the air gaps were assessed, by means of Monte Carlo (MC) simulations. Two methods of obtaining the magnetic field correction factor are presented and a rigorous analysis of the uncertainties is performed. The values of Farmer-type chamber magnetic field correction factors obtained in this work are compared with values from other studies, and may be used to support and extend existing data sets of correction factors, all with the aim of reducing the uncertainty in the measurement of absorbed dose to water for MRIgRT systems.

The application of work described in the current paper would include an alanine dosimetry service, for MRI-linac systems. This would allow the calibration of ionisation chambers either by a site visit to RT centres or as a postal dosimetry service. In the first case, NPL would perform measurements with alanine and its own fully calibrated instruments in order to determine absorbed dose to water and calibrate the user's ionisation chamber (s). In this case, traceability to the national standard is confirmed by an NPL calibration report. For the postal dosimetry service, alanine pellets loaded in Farmer-type holders are posted to the users of MRI-linacs, where they irradiate the alanine and post them back to NPL. NPL reports only the absorbed dose to water, which is traceable to the NPL primary standard. The latter case is mentioned here, but its implementation and use is not considered further in this paper.

2. Materials and methods

2.1. Traceable measurements of absorbed dose to water in magnetic fields

Traceability for measurements of the absorbed dose to water is usually achieved through utilisation of a transfer standard. A transfer standard is acting as a reference for calibrating secondary detectors (user detectors). The calibration is performed under reference conditions (i.e. source-to-detector distance, depth in water, field size, environmental conditions, etc.), which are the same conditions under which the absolute absorbed dose to water has been realised from a primary standard. If detectors are irradiated in some other conditions, then a correction should be applied to account for the resulting change in the detector signal.

A magnetic field will affect the value of the absorbed dose to water at the reference point. The magnetic field can also affect the detector signal, and these two effects are inseparable experimentally. Instead it is necessary to determine the effect on absorbed dose to water by other means, such as MC simulation, and to combine this effect with the empirically observed change in the detector signal, to obtain the magnetic field correction factor for the detector. The result is that the corrected detector signal relates to the value absorbed dose to water at the reference point, in the presence of the magnetic field.

The dissemination of the physical quantity absorbed dose to water, in the presence of a magnetic field, requires the use of a transfer standard, whose response has been corrected for any effects of the magnetic field, with an acceptably small uncertainty. The route that has been followed in this work uses alanine as a transfer detector, whose calibration is traceable to the NPL's primary standard of absorbed dose to water. A diagram of the route is given in figure 1, which shows the dissemination of absorbed dose to water from the primary standard to the end user of MRIgRT. First, alanine is calibrated against the NPL's primary standard (graphite calorimeter) at a 60 Co beam energy, under reference conditions and zero magnetic field. A beam quality correction factor, k_{Q,Q_0}^{al} , allows the use of alanine in different energy beams (e.g. clinical linac beams in conventional RT) and a magnetic field correction factor, k_{Q_B,Q_0}^{al} , allows for alanine measurements of absorbed dose to water in the presence of a magnetic field (i.e. MRIgRT). The result is a calibration of the user detector (field instrument) in terms of absorbed dose to water determined by direct comparison with the alanine

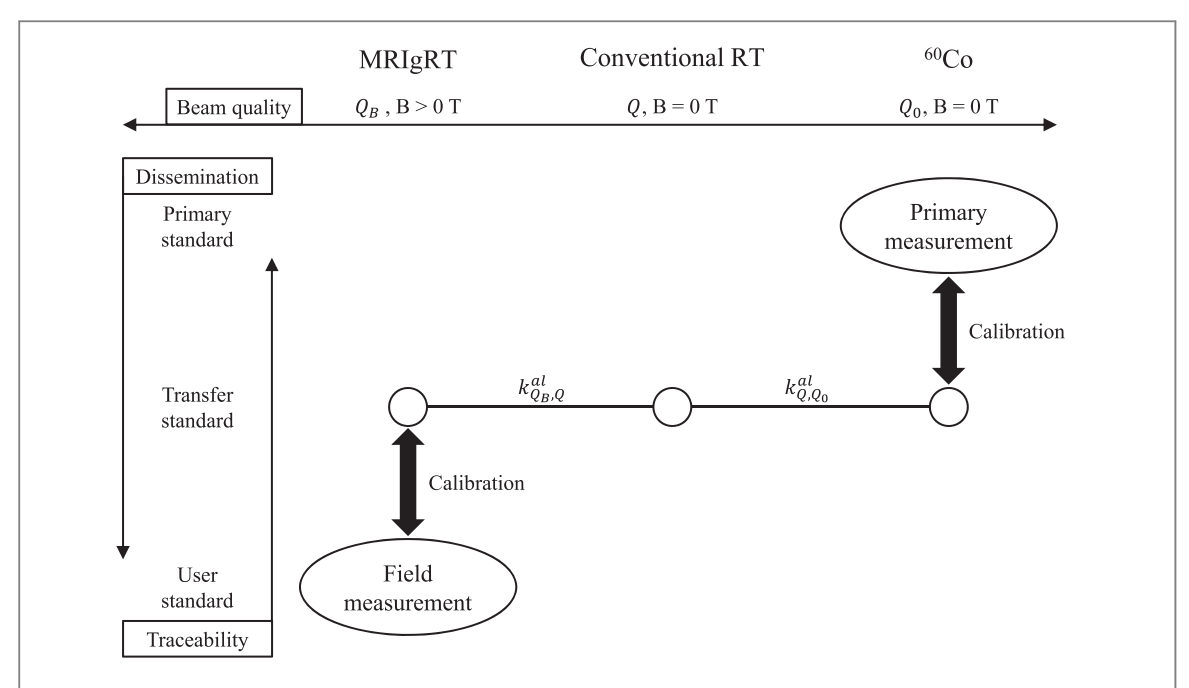


Figure 1. Traceability route for measurements of the absorbed dose to water in the presence of a magnetic field and for the calibration of a field instrument using alanine as a transfer standard.

detector, under reference conditions, in the MRI-linac. The use of $k_{Q_B,Q}^{al}$ is described in section 2.5 and k_{Q,Q_0}^{al} correction factor is explained in the following.

The absorbed dose to water response of alanine has a weak dependence on beam quality and alanine produces a slightly smaller electron paramagnetic resonance (EPR) signal for a given dose when irradiated by megavoltage x-rays compared to 60 Co irradiation. Investigation by various researchers (Bergstrand *et al* 2003, 2005, Sharpe 2003, Zeng *et al* 2004, Anton *et al* 2013) reported an average reduction of alanine response up to 0.8%. A study by Thomas *et al* (2014), which uses the alanine used in this study, has shown a correction of 1.004 \pm 0.006, and this is the value applied to correct the alanine energy dependence in this work.

2.2. Ionisation chamber calibration coefficient in magnetic fields

The calibration coefficient, N_{D,w,Q_B} , in terms of absorbed dose to water, D_w , for a beam quality Q, of an ionisation chamber in the presence of a magnetic field B, is given by:

$$N_{D,w,Q_B} = \frac{D_{w,Q_B}}{M_{Q_B}},\tag{1}$$

where, M_{Q_B} and D_{w,Q_B} are the corrected ionisation chamber signal and the absorbed dose to water, respectively, in the presence of a magnetic field. In this study, the absorbed dose to water under reference conditions, in the presence of a magnetic field, D_{w,Q_B} , is measured by using alanine (al) as a transfer standard:

$$D_{w,Q_B} = M_{Q_B}^{al} \cdot k_{Q_B,Q}^{al} \cdot k_{Q,Q_0}^{al} \cdot N_{D,w,Q_0}^{al} \cdot k_{vol}^{al},$$
(2)

where, $M_{Q_B}^{al}$ is the alanine/EPR signal in the presence of a magnetic field, $k_{Q_B,Q}^{al}$ is the alanine magnetic field correction factor, k_{Q,Q_0}^{al} is the alanine beam quality correction factor, N_{D,w,Q_0}^{al} is the calibration coefficient of the alanine detector at a 60 Co beam energy in the absence of a magnetic field and k_{vol}^{al} is the volume averaging correction factor on the alanine/EPR signal.

Equation (1) can be rewritten as follows, to consider the influence quantities that will perturb the signal from an ionisation chamber:

$$N_{D,w,Q_B} = \frac{M_{Q_B}^{al} \cdot k_{Q_B,Q}^{al} \cdot k_{Q,Q_0}^{al} \cdot N_{D,w,Q_0}^{al} \cdot k_{vol}^{al}}{M_{Q_Braw} \cdot k_{elec} \cdot k_{T_D} \cdot k_{ion} \cdot k_{vol}},$$
(3)

where:

 M_{Q_Braw} is the displayed chamber signal on the electrometer

 k_{elec} is the correction factor for the electrometer

 k_{Tp} is the correction factor for temperature and pressure

 k_{ion} is the correction factor for ion recombination

 k_{vol} is the correction factor for volume averaging

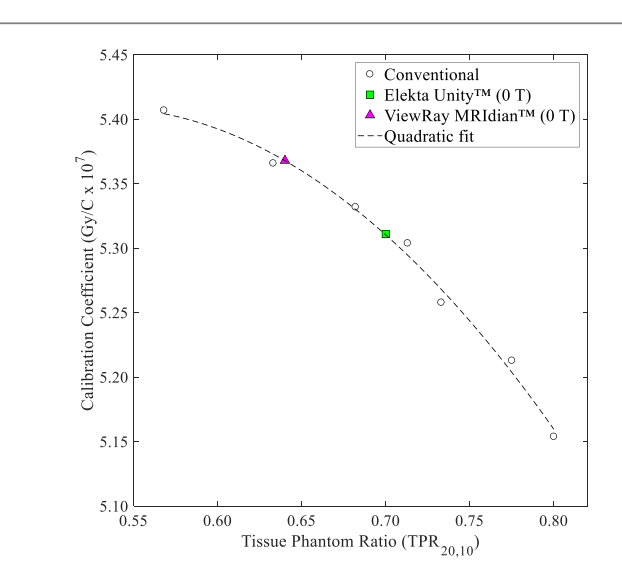


Figure 2. PTW 30013 Farmer-type chamber, with a serial number 3981, calibration coefficients as a function of beam quality index $(TPR_{20,10})$ in a conventional linac. The interpolated calibration coefficients of the Elekta UnityTM and the ViewRay MRIdianTM, both at 0 T, are also presented with a filled square and triangle marker, respectively.

In this work all readings are taken with the ionisation chamber operated at negative polarity, and these are the conditions under which the resulting calibration coefficients have been used. Previous work has shown that the polarity effect is small and independent of the magnetic field (de Prez et al 2019b).

2.3. Determination of the quality correction factor for the presence of a magnetic field on a radiation detector

The magnetic field correction factor, $k_{Q_B,Q}$, is required for the determination of the absorbed dose to water in the presence of a magnetic field, if the detector calibration coefficient is only available in the absence of any magnetic field. This factor corrects for the effect of the magnetic field on dose to water and also for the effect on the detector's response, and is defined as:

$$k_{Q_B,Q} = \frac{N_{D,w,Q_B}}{N_{D,w,Q}},$$
 (4)

where, $N_{D,w,Q}$ is the calibration coefficient in the absence of a magnetic field:

$$N_{D,w,Q} = \frac{D_{w,Q}}{M_Q},\tag{5}$$

In this work, $k_{Q_B,Q}$ was determined based on two different methods: one indirect and one direct, and these are explained in the following sections.

2.3.1. Indirect determination of $k_{O_{B},O}$

The experimental determination of the calibration coefficient at both 0 T and the MRI-linac field strength, implies that the magnetic field of the MRI scanner is off. However, the process of ramping down, and up, a superconducting magnet solely for the purpose of this measurement, is time consuming, expensive and impractical. An alternative, indirect, way to determine a calibration coefficient at zero magnetic field and at a beam quality of an MRI-linac, is described. This method has been presented by Billas *et al* (2017) and de Pooter *et al* (2021), but a more detailed explanation is given here. Provided that the chamber is calibrated at a range of megavoltage x-ray beams from a conventional linac and in 60 Co, for zero magnetic field, the calibration coefficient can be determined as a function of beam quality index, Tissue Phantom Ratio (TPR_{20,10}), and interpolated to the value measured in the MRI-linac. Figure 2 shows an example of an absorbed dose to water calibration coefficient as a function of TPR_{20,10} for a Farmer-type chamber. A quadratic fit is applied and the interpolated calibration coefficients of an Elekta UnityTM and a ViewRay MRIdianTM beam quality are shown with a filled square and a triangle marker, respectively. The calibration coefficient in the presence of a magnetic field can be obtained based on the method described in section 2.1.

Note that $TPR_{20,10}$ has been shown to be independent of the magnetic field (O'Brien *et al* 2016, van Asselen *et al* 2018), and as long as the field size is $10 \text{ cm} \times 10 \text{ cm}$ at the measurement plane, then $TPR_{20,10}$ is also independent of the source-to-detector distance (SDD). Consequently, the $TPR_{20,10}$ measured in MRI-linacs,

Table 1. Visited radiotherapy treatment centres, their operating MRI-linac systems and centres where measurements were performed at 0 T, while the magnet of the MRI scanner was switched off.

	MRI-		
Radiotherapy centre	Elekta Unity™ 1.5 T	ViewRAY MRIdian™ 0.35 T	Measurement at 0 T in MRI-linac
NKI	✓		
RMH/ICR	✓		✓
Christie	✓		✓
Odense	✓		✓
IPC		✓	✓
GCUK		✓	

NKI: Netherlands Cancer Institute, The Netherlands.

RMH/ICR: The Royal Marsden Hospital and The Institute of Cancer Research, UK.

Christie: The Christie NHS Foundation Trust, UK.

Odense: Odense University Hospital, Denmark.

IPC: Institute Paoli Calmettes, Marseille, France.

GCUK: GenesisCare, Oxford, UK.

with the magnet switched on, may be used to determine the calibration coefficient, at 100 cm SDD, at zero magnetic field as explained above. It is possible that the $TPR_{20,10}$ is affected by the magnetic field, but from the limited measurements performed in this study, this change cannot be quantified precisely. Instead, a contribution from this influence quantity has been included in the uncertainty analysis.

2.3.2. Direct determination of $k_{O_{B},O}$

In this work, the direct determination of $k_{Q_B,Q}$, was performed based on the calibration of the detectors directly in an MRI-linac in the presence and the absence of the magnetic field. The traceability route described in section 2.1 was used to obtain both calibration coefficients, but, when the magnet was switched off, the alanine magnetic field correction factor was omitted.

2.4. Measurements and experimental setup

Measurements were made in the MRI-linac facilities at six RT treatment centres (table 1). Four operate an Elekta Unity™ system and two a ViewRAY MRIdian™ system. Dose measurements were also performed while the constant magnetic field of the MRI scanner was off (0 T) at four of the six visited centres (table 1). The experimental setup, for both cases, includes irradiation of Farmer-type chambers (a PTW type 30013 and an IBA type FC65-G) and alanine dosimeters, which serve as the transfer standard. Dose measurements were performed in water, at the machine isocentre (143.5 cm for the Elekta Unity™ and 90 cm for the ViewRay MRIdian™), at a water-equivalent depth of $10\,\mathrm{g\,cm}^{-2}$ and a radiation field size of $10\,\mathrm{cm}\, imes10\,\mathrm{cm}$ at the measurement plane. The Farmer-type chamber long axis was orientated either parallel $(\uparrow\uparrow)^4$, anti-parallel $(\uparrow\downarrow)^5$ or perpendicular $(\bot)^6$ to the magnetic field and alanine always parallel (figure 3). The gantry angle was either 0° or 90° with the detector long axis always perpendicular to the radiation beam.

The use of six different MRI-linacs enabled an assessment of the consistency of the methodology followed in this work. The linac-to-linac variation may also be assessed, at least for the Elekta Unity™ system, since more than two machines were visited.

Alanine pellets were loaded in a waterproof holder of polyether ether ketone (PEEK) material shaped like a Farmer-type ionisation chamber. The measurement reference point of a Farmer-type chamber is very close to the centre of the third pellet from the tip of the holder. So, the average of five alanine pellets from the tip of the holder was used for the measurement of the absorbed dose to water.

Measurements were performed using a water tank, which was placed on the patient couch (figure 4) inside the bore of the MRI scanner. Two different water tanks were used throughout the measurements at the six RT centres:

 $^{^4}$ Parallel (↑↑): detector is pointing towards the front of the machine for Elekta Unity[™] and towards the back of the machine for ViewRay MRIdian™.

 $^{^{5} \, \}text{Anti-parallel ($\uparrow$$$$$$$$$): detector is pointing towards the back of the machine for Elekta Unity$^{\texttt{m}}$ and towards the front of the machine for Elekta Unity$^{\texttt{m}}$ and towards the front of the machine for Elekta Unity$^{\texttt{m}}$ and towards the first of the machine for Elekta Unity$^{\texttt{m}}$ and towards the first of the machine for Elekta Unity$^{\texttt{m}}$ and towards the first of the machine for Elekta Unity$^{\texttt{m}}$ and towards the first of the machine for Elekta Unity$^{\texttt{m}}$ and towards the first of the machine for Elekta Unity$^{\texttt{m}}$ and towards the first of the machine for Elekta Unity$^{\texttt{m}}$ and towards the first of the machine for Elekta Unity$^{\texttt{m}}$ and towards the first of the machine for Elekta Unity$^{\texttt{m}}$ and towards the first of the machine for Elekta Unity$^{\texttt{m}}$ and towards the first of the machine for Elekta Unity$^{\texttt{m}}$ and towards the first of the machine for Elekta Unity$^{\texttt{m}}$ and the first of the machine for Elekta Unity$^{\texttt{m}}$ and the first of the first$ ViewRay MRIdian™.

 $^{^{6}}$ Perpendicular (⊥): detector is pointing towards the bottom of the machine for both Elekta Unity[™] and ViewRay MRIdian[™].

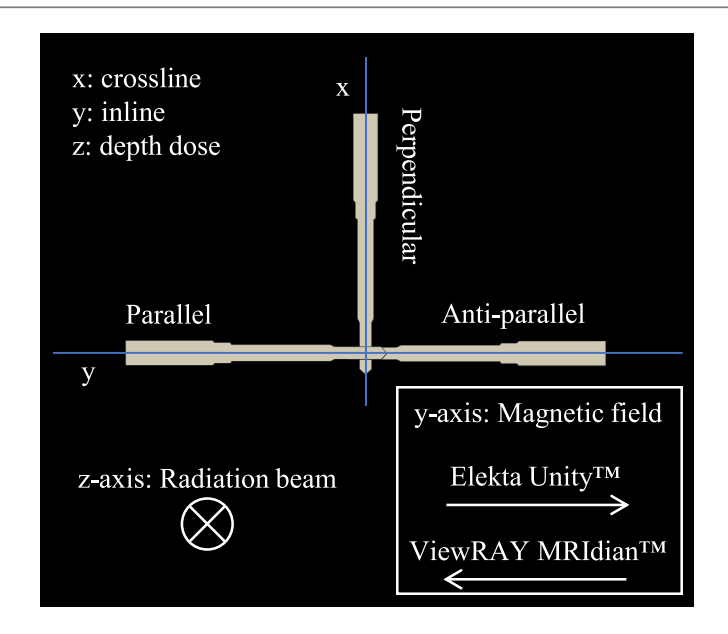


Figure 3. Orientations of a Farmer-type chamber and an alanine holder (shaped as a Farmer-type chamber) with respect to the magnetic field and the radiation beam. The crossline and inline profiles are across x- and y-axis, respectively, and depth dose in z-axis. Symbol \otimes indicate magnetic field pointing into the plane.



Figure 4. Experimental setup on the Elekta Unity™ (left) and the ViewRay MRIdian™ (right).

- 1. A PTW MP1 1D manual water tank was used for measurements at NKI and The RMH/ICR. A polymethyl methacrylate (PMMA) holder that could accommodate the detectors was fixed to a manual stepping mechanism enabling the crossline movement. For this setup, measurements were performed with the detector long axis orientated anti-parallel to the magnetic field and perpendicular to the radiation beam.
- 2. An NPL in house developed water tank, with dimensions of 33.0 cm width, 33.0 cm length and 21.5 cm height, was used for measurements at The Christie, Odense, IPC and GCUK. The water tank consists of PMMA and includes a square frame, which is constructed such that the detector long axis is orientated either parallel, anti-parallel or perpendicular to the magnetic field, by maintaining the same chamber reference point. In all three orientations the chamber long axis was perpendicular to the radiation beam.

In the Elekta UnityTM system, the machine isocentre was defined based on the central pixel (iso-pixel) of 2D MV planar images using an electronic portal imaging device. Images were acquired with the gantry angle being 0° and 90° . The chamber cavity was aligned so that the iso-pixel, in images from both gantry angles, is shown at the measurement reference point of the chamber. In the ViewRay MRIdianTM system, a practical isocentre was defined based on room lasers outside of the bore, which is positioned approximately 155 cm from the machine isocentre.

Each Farmer-type chamber was connected to a calibrated electrometer and measurements were performed with beam deliveries of 200 MU, collecting negative charge (between -30 and -40 nC, depending on the MRI-linac system and chamber orientation). Before each measurement, the electrometer was warmed-up, as required, and zeroed to account for any background noise. The relative humidity was monitored to be between 20% and 70% and the collected charge was corrected to standard environmental conditions (20 °C and 1013.25 hPa). Ambient air pressure was measured by using a calibrated barometer and temperature was measured with a calibrated alcohol thermometer placed in the water tank.

A correction for the incomplete collection of charge due to ion recombination, k_{ion} , was measured and applied, for all three chamber orientations with respect to the magnetic field. By assuming that the ion recombination is less than 3%, the two-voltage method (Boag and Currant 1980) was a good approximation (within 0.1%) to determine k_{ion} (Andreo *et al* 2000). To further validate this method, Jaffé plots for a PTW 30013 and an IBA FC65-G chamber were performed directly in an Elekta UnityTM at 1.5 T. A linear dependence of 1/M on 1/V, for both chambers, was found but the details are omitted from this paper.

Correction factors due to volume averaging, k_{vol} , for alanine and Farmer-type chambers were determined, considering the dimensions of their collecting volume and the flattening filter free (FFF) beams of the MRI-linac systems. Correction factors were defined based on the equation 54 in TRS 483 (Palmans *et al* 2017).

The measurement sequence includes a set of five irradiations for each Farmer-type chamber. The readings of each set were examined to confirm no trend and that the standard deviation of the mean was less than 0.05%. Several alanine dosimeters were irradiated to a nominal dose of 20 Gy in between the chamber irradiations. The behaviour of the linac output was monitored by including a chamber (acting as a monitor) several times in between the detectors irradiation and always in one orientation. Any deviation that occurred was used to correct the absorbed dose to water, measured with alanine, at the chamber irradiation time.

The beam quality index was based on TPR $_{20,10}$ measurements in water. As recommended by TRS 398 (Andreo *et al* 2000) water-equivalent depths of 10 and 20 g cm $^{-2}$ were used, with the source-to-chamber distance being fixed and always at one orientation. Chamber readings were corrected for ion recombination and to standard air density.

The alanine dosimetry system, as well as the PTW 30013 and IBA FC65-G Farmer-type chambers, used in this study were calibrated at NPL based on the Code of Practice for high energy photon therapy dosimetry (Lillicrap *et al* 1990, Eaton *et al* 2020). The calibration was performed in a conventional Elekta Synergy linac (zero magnetic field), for a range of megavoltage x-ray beams between 4 and 18 MV, and in ⁶⁰Co radiation, collecting negative charge (for the chambers), traceable to the NPL primary standard of absorbed dose to water. The PTW 30013 and IBA FC65-G Farmer-type chambers calibration coefficients obtained at NPL, together with those of an MRI-linac, could indirectly determine magnetic field correction factors, as explained in section 2.3.1.

2.5. Alanine magnetic field correction factor, $k_{Q_BQ}^{al}$

The magnetic field affects the determination of absorbed dose to water using alanine in multiple ways: it modifies the dose to water, but it also modifies the absorbed dose sensitivity to the alanine itself. By considering the intrinsic sensitivity of the alanine, $F_{Q_B,Q}$, i.e. its response relative to the absorbed dose to alanine, rather than to the absorbed dose to water, the alanine sensitivity was shown in our previous published study (Billas *et al* 2020) to be independent of the beam energy. This alanine intrinsic sensitivity, previously determined, was combined with MC simulations of absorbed dose to water and of absorbed dose to alanine for the experimental setups used in the present study, to obtain the required magnetic field correction factor for alanine, $k_{Q_B,Q}^{al}$.

The effect of the magnetic field on the absorbed dose, to water and to alanine, depends on the field strength and on the beam energy. Therefore, MC simulations were performed to calculate the absorbed dose, to water and to alanine, with and without a magnetic field for the beam energies and the magnetic field strengths of the Elekta Unity™ and the ViewRay MRIdian™ systems. Simulations were also performed for the uncertainty estimation due to the air gaps associated with the alanine holder. We refer the readers to Billas *et al* (2020) for a detailed explanation on the MC simulations and the transport parameters used in the present study (i.e. models of the alanine pellet and its holder, ECUT, PCUT, EM ESTEPE, etc). The sections 2.5.1 and 2.5.2 describe the MC simulations of the beam models of the two MRI-linac systems and the experimental setup performed to validate them. The *cavity* and the BEAMnrc user codes, that forms part of the EGSnrc code system (Kawrakow *et al* 2011), were used for the MC simulations in this work.

2.5.1. MC simulations of the MRI-linac beam models

An accurate beam model will determine the quality and the accuracy of a calculated alanine magnetic field correction factor, which is needed for the determination of the absorbed dose in the presence of a magnetic field. Phase space data of the Elekta UnityTM were provided by Elekta. The beam was modelled to generate phase space files at a distance plane of 129.5 cm form the source. This provides a $10 \text{ cm} \times 10 \text{ cm}$ radiation field at the isocentre plane (143.5 cm).

Table 2. Alanine magnetic field correction factors, $k_{QB,Q}^{al}$, for the Elekta Unity[™] and the ViewRay MRIdian[™] systems together with the alanine relative intrinsic sensitivity values, $F_{QB,Q}$, and the calculated ratios of absorbed dose to water (with and without magnetic field) and ratios of absorbed dose to alanine (without and with magnetic field). The uncertainties shown are standard uncertainties (k = 1).

	$F_{Q_B,Q}$	$D_{w,Q_B}/D_{w,Q}$	$D_{al,Q}/D_{al,Q_B}$	$k_{Q_B,Q}^{al}$	
Elekta Unity TM ViewRay MRIdian TM	$\begin{array}{c} 1.0071 \pm 0.0008 \\ 1.0016 \pm 0.0002 \end{array}$	$\begin{array}{c} 0.9950 \pm 0.0012 \\ 1.0001 \pm 0.0012 \end{array}$	$\begin{array}{c} 1.0077 \pm 0.0017 \\ 1.0012 \pm 0.0017 \end{array}$	$0.9957 \pm 0.0059 \\ 0.9997 \pm 0.0028$	

An accelerator head model of the ViewRay MRIdian™ was built using the BEAMnrc user code. Taking the best approach, the model was constructed by using dimensional details and material specifications taken from the literature (Mutic and Dempsey 2014, Kluter 2019) and information found on the manufacturer's website. Important features which are critical for an effective beam model are:

- the distance from the source-to-isocentre, 90 cm, and the distance from the isocentre to the distal side of the multi-leaf collimator (MLC), 50.5 cm
- the double-stack and double-focus MLC (without additional jaws) which comprises of 34 leaf pairs on the upper stack and 35 leaf pairs on the lower stack, with each leaf having a physical width and height of 0.4 cm and 5.5 cm, respectively
- the minimum, 0.2 cm \times 0.415 cm, and the maximum, 24.1 cm \times 27.4 cm, radiation field sizes at the isocentre

There was no need to model any of the MRI components (i.e. cryostat, gradient coil, etc.), as the beam is passing through the 28 cm gap, between the two superconducting magnet halves, and only attenuated by a 0.5 cm thick connecting fibreglass panel (Kluter 2019).

On simulating the ViewRay MRIdianTM beam, the BEAMnrc model was compiled as a shared library and used as a direct input for dose calculations in the *cavity* user code. In this method, both user codes will run in parallel, which will make the simulations more efficient and provide better uncertainties on dose calculations, compared with generating phase space files.

The elliptical beam with gaussian distribution in x and y (ISOURCE = 19) was used to simulate the primary electron beam. The ellipse was specified by the full width at half maxima of the energy distributions in x = 0.11 cm) and y = 0.11 cm). An electron energy spectrum from an in house 6 MV FFF beam model was used for the simulations. The energy tuning was performed by simulating a 10 cm \times 10 cm radiation field using the electron spectrum with varying mean energies in the range of 5.3 to 7.7 MeV in steps of 0.4 MeV.

2.5.2. Validation of the virtual beams

The phase space file provided by Elekta to represent the beam from a Unity™ MRI-linac, and the beam model developed to represent the ViewRay MRIdian™, were validated by comparing MC calculated lateral and depth dose profiles with measured data (see figure 3 for the direction of the profiles with respect to the magnetic field and the radiation beam). The experimental setup involves a scan of a 10 cm × 10 cm radiation field, in a water tank, using a PTW 60019 microdiamond detector. The detector was positioned vertically (parallel to the radiation beam), the source-to-surface distance was 133.5 cm (Elekta Unity™) and 80 cm (ViewRay MRIdian™) and the inline and crossline profiles at a mass depth of 10 g cm⁻² were acquired. For the Elekta Unity™ the measurements were performed in Odense and for the ViewRay MRIdian™ data were provided from GCUK.

3. Results

3.1. Alanine magnetic field correction factor, $k_{O_{R},O}^{al}$

Table 2, contains results for the alanine relative intrinsic sensitivity values, $F_{Q_B,Q}$, the MC calculated ratios of absorbed dose to water (with and without magnetic field) and ratios of absorbed dose to alanine (without and with magnetic field), and the alanine magnetic field correction factors, $k_{Q_B,Q}^{al}$, for the Elekta UnityTM and the ViewRay MRIdianTM systems. The combined standard uncertainties on the $k_{Q_B,Q}^{al}$ values include the uncertainty due to the air gaps, as well.

The validation of the virtual beams and the MC simulations performed for the uncertainty estimation due to the air gaps, are described in sections 3.1.1 and 3.1.2.

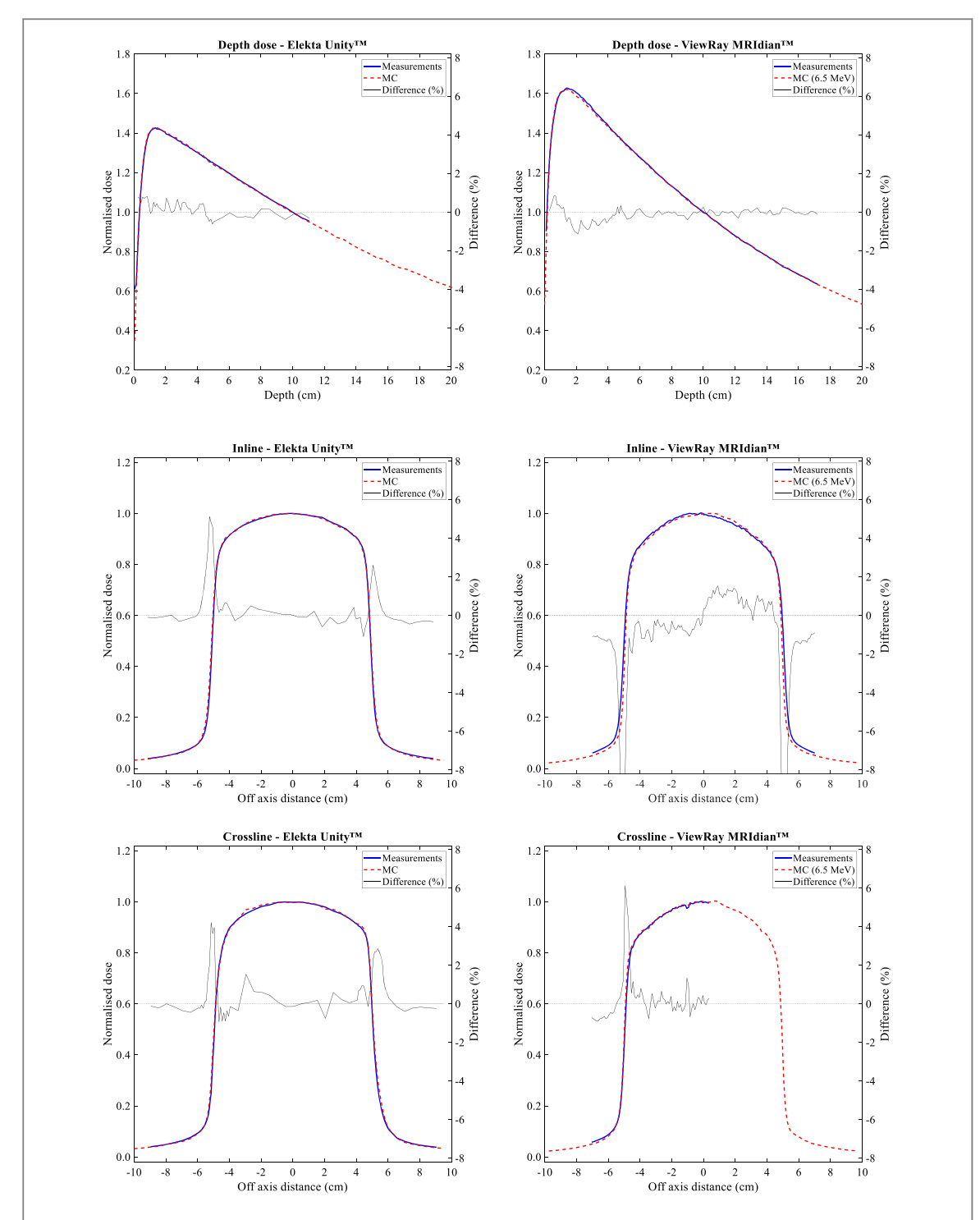


Figure 5. Measured and MC calculated lateral (inline and crossline) and depth dose profiles of the Elekta UnityTM and the ViewRay MRIdianTM (electron energy of 6.5 MeV) radiation beams. The percentage dose difference relative at the maximum dose of the measured profiles is shown in the right y-axis of each plot. Note that for the benefit of enhancing the percentage dose difference on the right y-axis of each plot, the scale is set to $\pm 8\%$. The value of the Inline - ViewRay MRIdianTM reaches down to -16%.

3.1.1. Validation of the virtual beams

The Elekta UnityTM phase space file and the ViewRay MRIdianTM beam model were validated by comparing MC calculated lateral (inline and crossline) and depth dose profiles with measured data, as shown in figure 5. To enable a comparison in terms of dose differences the MC calculated data were interpolated to the measured depth and off-axis distance points using piecewise cubic Hermite polynomial functions (which preserves the shape of the data). The measured and the MC fit lateral dose profiles were normalised to the central axis and the depth dose profiles at 10 cm depth. In the right y-axis of each plot in figure 5, the percentage dose difference relative at the maximum dose of the measured profiles is shown.

For the Elekta UnityTM, the dose agreement at each point is generally within $\pm 1\%$, except two regions confined to the steepest parts of the penumbra, where the dose difference varied over a range of 5%. It should be

Table 3. Statistics of the absolute value of the difference between the measured and MC normalised depth doses of the different electron energies, for the ViewRay MRIdian™.

Electron energy (MeV)	Absolute difference in norm ised depth dose				
Electron energy (MeV)	Standard deviation	Mean			
5.3	0.0293	0.0230			
5.7	0.0189	0.0135			
6.1	0.0107	0.0073			
6.5	0.0088	0.0055			
6.9	0.0145	0.0124			
7.3	0.0209	0.0185			
7.7	0.0285	0.0254			

possible to substantially reduce these differences by making a very small adjustment to the collimator setting, however, for the present investigation in which the reference dose measurements are all close to the central axis, this adjustment is not essential.

For fine tuning the energy on the ViewRay MRIdianTM beam model, depth dose profiles were calculated by MC simulation for various electron energies in the range from 5.3 to 7.7 MeV. The electron energy was chosen to optimise the agreement between MC calculated and measured normalised depth doses, based on the statistics of the absolute value of their difference. The mean and standard deviation are shown in table 3 for the seven energies simulated, and 6.5 MeV is the energy which produces the best agreement. Figure 5 shows MC calculated and measured lateral and depth dose profiles of the ViewRay MRIdianTM with this optimum electron energy of 6.5 MeV. There is a small discrepancy outside the primary beam, beyond the steep part of the penumbra, between the calculated and the measured lateral dose profiles. This might be due to an incompleteness (i.e. missing components) in the linac geometry used to generate beams for this study. Another aspect of the observed difference in the inline profiles is a lack of symmetry, predominantly of the measured profile (the MC simulation is symmetric, and any asymmetry should only be the result of random uncertainty). Nevertheless, restricting the comparison in the area where the alanine simulations take place (within ± 4.5 cm from the central axis), the calculated inline and crossline profile data agree very well with measurements with the dose agreement at each point being less than $\pm 1.4\%$. Note that practical limitations in the experimental setup meant that the crossline profile could only be accurately measured up to approximately 5 mm beyond the central axis.

3.1.2. Validation of the model: experimental setup and alanine air gap effect

The model of the experimental setup (including alanine dosimeter and holder) were validated with measurements in a similar way as was done in Billas $et\ al\ (2020)$, but in the radiation fields and magnetic field configurations of the Elekta UnityTM and the ViewRay MRIdianTM systems.

MC simulations were also performed to investigate the effect of the air gaps formed due to the unknown spatial distribution of the pellets in the holder, similarly to our previous study (Billas *et al* 2020). This effect is included among the influence quantities considered in the uncertainty analysis. Simulations were performed to include beam energies of the Elekta UnityTM and the ViewRay MRIdianTM systems and reflect the experimental setup (the holder orientated parallel to the magnetic field and perpendicular to the radiation beam). The RMS (root mean sqaure) variation of the MC dose to alanine, arising from uncertainty in the positioning of the alanine pellets inside the holder, was found to be 0.55% and 0.17% for the Elekta UnityTM and the ViewRay MRIdianTM, respectively.

3.2. TPR_{20,10} of MRI-linacs

The measured beam quality index values, based on $TPR_{20,10}$, at all MRI-linac machines are shown in figure 6, which also includes $TPR_{20,10}$ values for 0 T. On average, $TPR_{20,10}$ for the Elekta UnityTM machines was found to be 0.700 ± 0.002 and 0.697 ± 0.003 for 0 T and 1.5 T, respectively. The $TPR_{20,10}$ of the ViewRay MRIdianTM was 0.645 for 0 T and 0.642 for 0.35 T (average of two values).

For both MRI-linac systems, there is a difference of 0.003 between the $TPR_{20,10}$ values without and with a magnetic field. Based on the Elekta UnityTM measurements, $TPR_{20,10}$ can vary up to 0.5% between different machines of the same type at 1.5 T. This variation will also include the setup repeatability on $TPR_{20,10}$ measurements. In this study, any difference observed between the $TPR_{20,10}$ without and with a magnetic field, may be within the variation of the $TPR_{20,10}$ between the different MRI-linac machines.

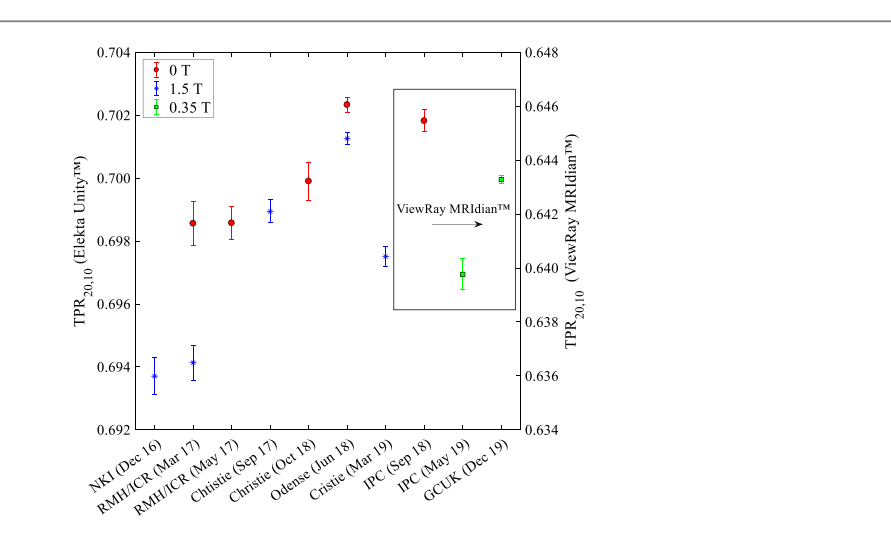


Figure 6. Measured TPR_{20,10} of the Elekta UnityTM (left *y*-axis) and the ViewRay MRIdianTM (right *y*-axis) without and with magnetic fields.

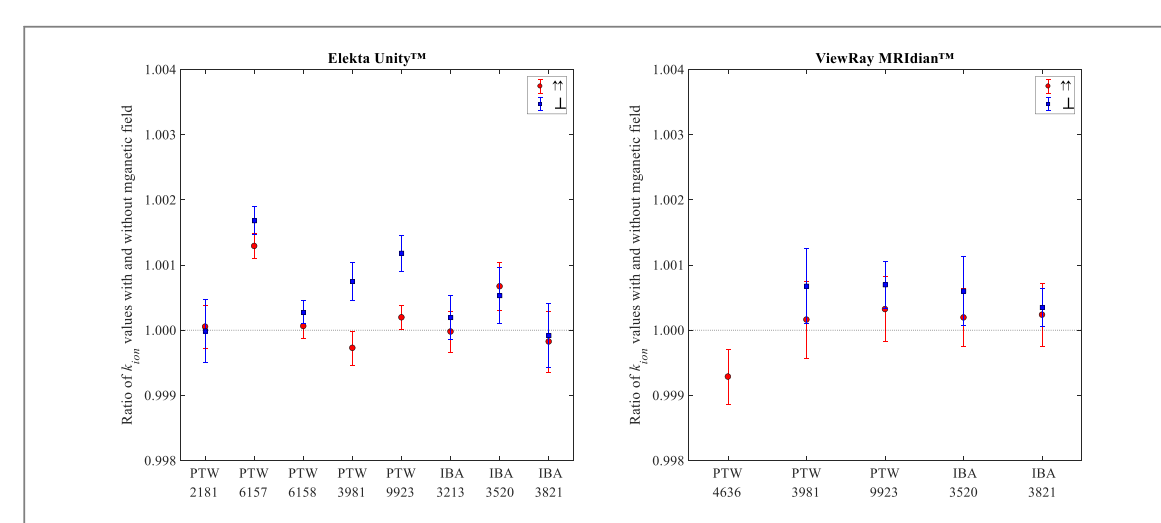


Figure 7. Ratios of k_{ion} values with and without magnetic field, of different PTW 30013 and IBA FC65-G Farmer-type chambers for the Elekta UnityTM and the ViewRay MRIdianTM. Data include results for parallel and perpendicular orientations. The four-digit numbers on the *x*-axes are the serial numbers of the ionisation chambers. Note that for the determination of the k_{ion} the operating/lower voltage was 400 V/150 V for the chambers with serial numbers 2181,6157,6158 and 4636. For the 3213 chamber was 300 V/100 V and for the rest of the chambers was 250 V/100 V.

3.3. Ion recombination correction factors, k_{ion}

The impact of the magnetic field on the ion recombination correction is typically small and is indicated in figure 7, which shows the ratio of the correction with, and without, the magnetic field. Results are shown for the chambers at the users' normal operating voltages: the ratio is generally slightly larger than unity, but with a noticeable intra-type variation for both MRI-linac systems. Data include results from two different chamber orientations with respect to the magnetic field, parallel and perpendicular. The correction factors are the results of measurements from one machine for each system (Odense for Elekta UnityTM and IPC for ViewRay MRIdianTM), when the constant magnetic field was off and on. Error bars represent the combined standard uncertainty of the collected charge at the operating polarising voltage and the collected charge at a lower voltage.

3.4. Volume averaging correction factors, k_{vol}

Figure 8 shows the measured lateral inline profiles of the Elekta UnityTM and the ViewRay MRIdianTM of a 10 cm \times 10 cm radiation field at the measurement plane, as described in section 2.5.2. Profiles are focused in an area of \pm 3 cm to show the non-uniformity of the two profiles, where a quadratic fit (solid lines) is also applied. The collecting volume of the alanine and the Farmer-type chamber, on their long axis, is also depicted and is indicating how the dose is distributed along their collecting volume. Following suggestions from TRS 483 (Palmans *et al* 2017), k_{vol} for the Elekta UnityTM was 1.0005 and 1.0019 for alanine and Farmer-type chamber,

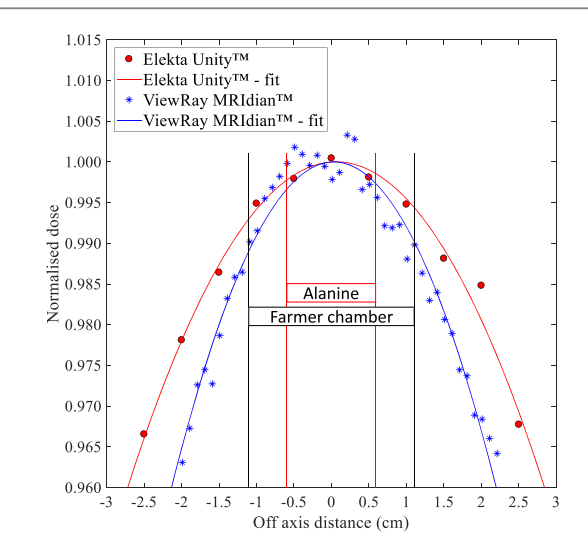


Figure 8. Measured lateral inline profiles of the Elekta Unity[™] and the ViewRay MRIdian[™] of a 10 cm \times 10 cm radiation field at the measurement plane (focus in an area of \pm 3 cm). A fit between the measured data points is applied and the collecting volume of the alanine and the Farmer-type chamber, on their long axis, is also depicted.

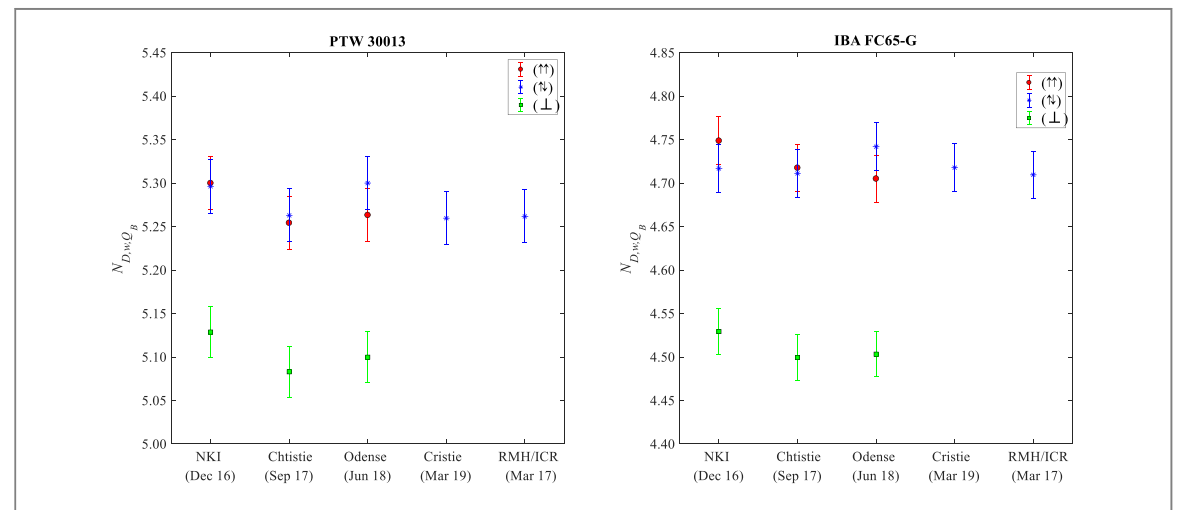


Figure 9. Farmer-type calibration coefficients for PTW 30013 (sn 3981) and IBA FC65-G (sn 3520), for the three orientations, at Elekta Unity™ machines and different centres, with the magnet switched on. Correlated contributions to the indicated uncertainty bars have been removed for the purpose of this comparison and the remaining standard uncertainty, 0.58%, is dominated by the effect of air gaps inside the alanine holder.

respectively. For the ViewRay MRIdianTM, k_{vol} was 1.0007 and 1.0028 for alanine and Farmer-type chamber, respectively. The type B standard uncertainty for all four values was estimated to be 0.05%.

A study by de Prez *et al* (2019b) found a difference of 0.02% on the k_{vol} values with and without a magnetic field and no significant difference between the k_{vol} values determined using the inline and the crossline profiles, in a magnetic field. Therefore, where applicable, the present study used the k_{vol} values as obtained above to correct the alanine/EPR and Farmer-type chamber signals.

3.5. Reference dosimetry measurements and calibration coefficients of Farmer-type chambers

Reference dosimetry measurements were performed at the visited centres (table 1) using the traceability route developed in this work. Absorbed dose to water was measured with alanine and the relative standard deviation of the pellet dose values was found, on average, to be 0.50% and 0.29% for Elekta UnityTM and ViewRay MRIdianTM machines, respectively. The difference in repeatability between the two machine types is in accord with the magnetic field strength dependence of the air gap uncertainty reported by Billas $et\ al\ (2020)$.

Figure 9 shows the calibration coefficients of two Farmer-type chambers, a PTW 30013 (serial number (sn) 3981) and an IBA FC65-G (sn 3520). These two chambers were calibrated at different Elekta Unity™ machines at three (or more) different centres, for the three orientations. Differences between the calibration coefficients, for each chamber orientation, are consistent within the standard uncertainties shown. Each calibration coefficient is

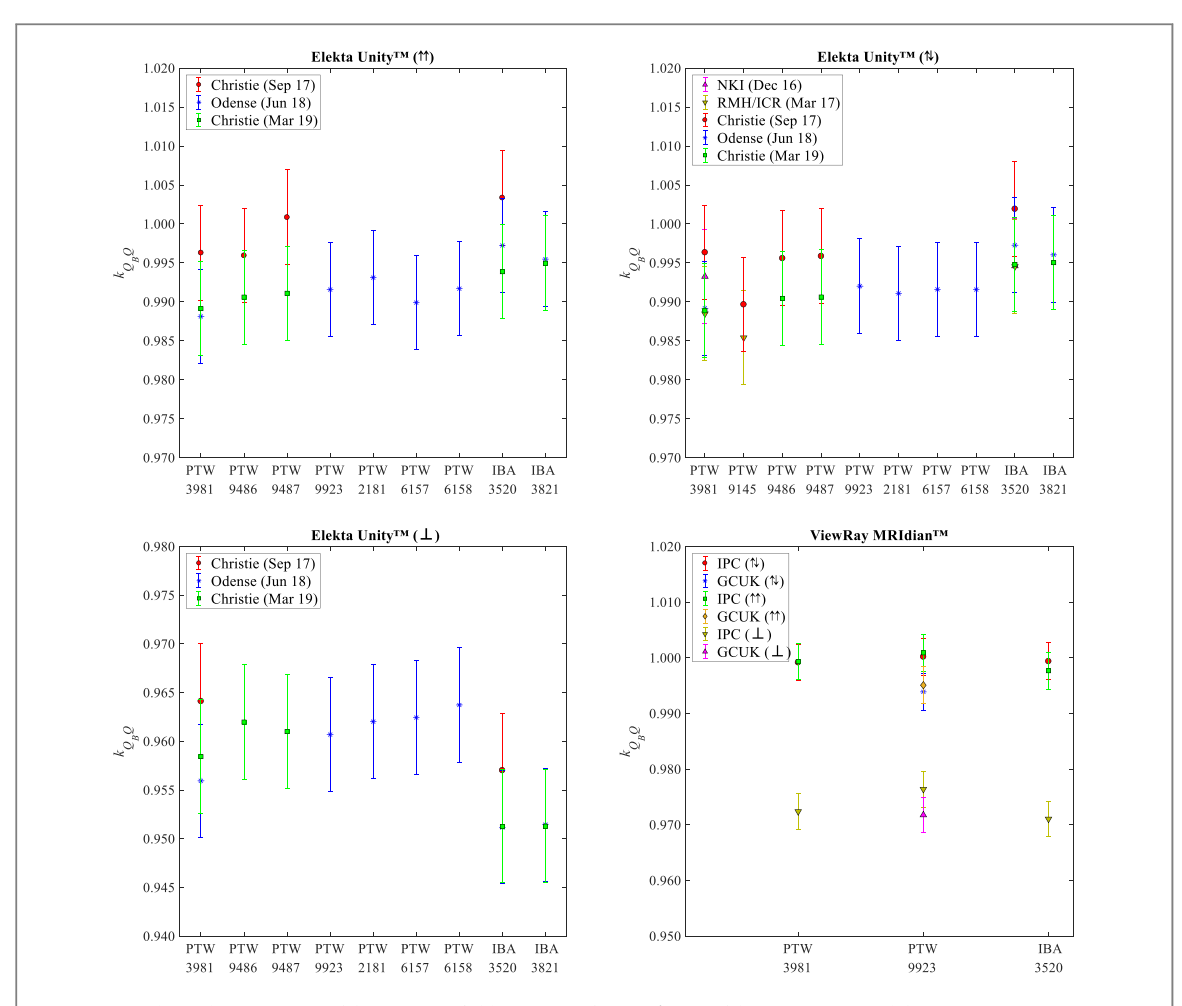


Figure 10. Indirect determination of the magnetic field correction factors, $k_{Q_B,Q}$, of the PTW 30013 and the IBA FC65-G Farmer-type chambers at different MRI-linac centres. Results are shown when the chamber long axis is orientated parallel, anti-parallel and perpendicular to the magnetic field of the Elekta UnityTM and the ViewRay MRIdianTM. The four-digit numbers on the x-axes are the serial numbers of the ionisation chambers. Correlated contributions to the indicated uncertainty bars have been removed for the purpose of this comparison and the remaining standard uncertainty is of the order of 0.61% and 0.33% for the Elekta UnityTM and the ViewRay MRIdianTM, respectively.

plotted with its standard uncertainty, but the contributions to uncertainty that would be correlated have been removed for the purpose of this comparison. Excluding correlations in this way reduces the combined standard uncertainty for each calibration coefficient from 1.06% to 0.58%. Results also indicate the degree of consistency of the reference dosimetry measurements performed in this work.

3.6. Farmer-type chamber magnetic field correction factors, $k_{Q_B,Q}$

Figure 10 shows results of the indirect determination of the magnetic field correction factors, $k_{Q_B,Q}$, of the PTW 30013 and the IBA FC65-G Farmer-type chambers at different MRI-linac centres. Results are shown when the chamber long axis is orientated parallel, anti-parallel and perpendicular to the magnetic field of the Elekta UnityTM and the ViewRay MRIdianTM systems. In the appendix, the indirect (table A1) and the direct (table A2) $k_{Q_B,Q}$ values of the PTW 30013 and the IBA FC65-G Farmer-type chambers for all visited centres, for both MRI-linac systems, are shown. Results are presented for the three orientations of the chamber with respect to the magnetic field ($\uparrow\uparrow$, $\uparrow\downarrow$, \bot). The standard uncertainty of each $k_{Q_B,Q}$ value is 0.88% for Elekta UnityTM and 0.71% for ViewRay MRIdianTM in the indirect method. For the direct method, the uncertainty is reduced to 0.62% and 0.34% for Elekta UnityTM and for ViewRay MRIdianTM, respectively. This is because the chambers were calibrated against alanine in the presence and the absence of a magnetic field, and any correlated uncertainties were not included.

3.7. Uncertainty budget

The analysis of uncertainty here follows the Joint Committee for Guides in Metrology (JCGM) Guide to the Expression of Uncertainty in Measurement (JCGM 2008). Uncertainties evaluated by statistical analysis are grouped as type A and the rest are grouped as type B. These are added in quadrature to give a combined standard uncertainty with coverage factor k=1.

Table 4. Uncertainty budget for the Farmer-type chamber calibration coefficient in the presence of a magnetic field for the Elekta Unity[™] and the ViewRay MRIdian[™] systems. Where it is not specifically stated (i.e. footnotes 7 and 8 cross-reference to the Elekta Unity[™] and the ViewRay MRIdian[™], respectively), uncertainties are the same for both MRI-linac systems.

	Relati	ve standard und	certainties
Uncertainty component	Type A (%)	Type B (%)	Combined (%
Uncertainties of the correction factors and quantities for the determination of absor-			
bed dose to water in magnetic field, D_{w,Q_B} , using alanine as a transfer standard.			
Alanine air gap effect	$0.55^7/0.17^8$	_	
Alanine relative intrinsic sensitivity, $F_{Q_B,Q}$		$0.08^7/0.02^8$	
Ratio of MC calculated absorbed dose to water with and without magnetic	0.07	0.10	
field, $D_{w,Q_B}/D_{w,Q}$			
Ratio of MC calculated absorbed dose to alanine without and with magnetic	0.14	0.10	
field, $D_{al,Q}/D_{al,Q_B}$			
Standard uncertainty in alanine magnetic field correction factor, $k_{OR,O}^{al}$			$0.59^7/0.28^8$
Alanine/EPR signal, M_{OR}^{al}	_	0.08	
Alanine beam quality correction factor, k_{O,O_0}^{al}	_	0.60	
Alanine calibration coefficient at 0 T in a ⁶⁰ Co energy beam	_	0.60	
Alanine volume averaging correction factor, k_{vol}^{al}		0.05	
Correction due to linac drift	0.06	_	
Standard uncertainty in D_{w,Q_B}			$1.04^7/0.90^8$
Uncertainties of the correction factors and quantities on the obtained chamber signal			
Raw chamber readings, M_{Q_Braw}	0.03	_	
Electrometer correction factor, k_{elec}	_	0.10	
Temperature	_	0.10	
Pressure	_	0.02	
Ion recombination correction factor, k_{ion}	0.04	_	
Farmer-type chamber volume averaging correction factor, k_{vol}		0.05	
Standard uncertainty in chamber signal, M_{Q_B}			0.16
Measurement repeatability	0.10	_	0.10
Overall combined relative standard uncertainty in the Farmer-type chamber calibra-			$1.06^7/0.92^8$

The quoted relative standard uncertainties are shown in table 4. The overall combined relative standard uncertainty in the chamber calibration coefficient in the presence of a magnetic field, N_{D,w,Q_B} , was found to be 1.06% for the Elekta UnityTM and 0.92% for the ViewRay MRIdianTM, with a coverage factor of k = 1. The uncertainty budget also reports uncertainties for the alanine magnetic field correction factor, $k_{Q_B,Q}^{al}$, $(0.59\%^7/0.28\%^8)$ and the absorbed dose to water in the presence of the magnetic field $(1.04\%^7/0.90\%^8)$. In table 4, where it is not specifically stated (i.e. footnotes 7 and 8 cross-reference to the Elekta UnityTM and the ViewRay MRIdianTM, respectively), uncertainties are the same for both MRI-linac systems.

The short-term behaviour of the output from the beams of each MRI-linac systems was recorded during the measurements over one day (see section 2.4). For each day of irradiation, the output (dose per MU) was found to decrease by 0.03%, or less, per hour. This deviation was considered, and used to correct the absorbed dose to water, measured with alanine, based on a linear fit between the ionisation chamber signal and the irradiation time. The uncertainty was estimated from the gradient of the residuals of the fit (RMS variation) and found to be 0.06%, on average.

In the MC simulations, the Type A uncertainties in the determination of the absorbed dose to water and to alanine, with and without a magnetic field, were less than 0.1%. For self-consistency and transport parameters a Type B uncertainty of 0.1% was estimated (Kawrakow 2000, Malkov and Rogers 2016). The combined standard uncertainty on the MC simulations resulted in less than 0.15%.

The uncertainty associated with the calibration of the alanine dosimeters in 60 Co energy beam, N_{D,w,Q_0}^{al} , and the uncertainty associated with the variation between individual dosimeter pellets have been determined by statistical methods, from the NPL chemical dosimetry laboratory, and are 0.6% and 0.3%, respectively. The latter results in a standard uncertainty of the mean alanine/EPR signal of 0.08%, considering fifteen pellets (irradiation of three alanine holders per measurement day). The uncertainty of the alanine beam quality

 $^{^{7}}$ Elekta Unity[™].

⁸ ViewRay MRIdian™.

correction factor, k_{Q,Q_0}^{al} (0.6%), together with the uncertainty of N_{D,w,Q_0}^{al} are the dominant components in the uncertainty budget.

The average charge over five irradiations for each Farmer-type chamber was used for the determination of each calibration coefficient. The standard deviation of the mean of the five charge readings, results in 0.03%, or less.

The uncertainty on the ion recombination correction factor, k_{ion} , was estimated to be 0.04%. This is based on the combined standard uncertainties of the chamber signal at the normal operating voltage and the chamber signal at a reduced voltage.

4. Discussion

A methodology for the traceable calibration of ionisation chambers in the presence of a magnetic field has been presented. This methodology uses alanine to calibrate ionisation chambers directly in MRI-linac systems. Alanine is calibrated against the NPL primary standard in zero magnetic field and its response is corrected for use in a magnetic field (Billas *et al* 2020). This approach was followed in six different centres that have MRI-linac systems (either an Elekta Unity™ or a ViewRay MRIdian™) and the results presented. Correction factors to realise the absorbed dose to water in the presence of a magnetic field have been evaluated and applied for both alanine and ionisation chambers. An indirect determination of the magnetic field correction factor for ionisation chambers, described in section 2.3.1, is also presented.

4.1. MC simulations and the alanine magnetic field correction factor

MC simulations were performed to support the determination of the alanine magnetic field correction factor for the two MRI-linac systems. The Elekta Unity™ phase space data (provided by Elekta) and the ViewRay MRIdian™ accelerator model (constructed by using dimensional details and material specifications found in the literature) were validated by comparing MC calculated lateral and depth dose profiles with measured data. The comparison was quantified using point dose differences between the measured and the calculated lateral and depth dose profiles.

The experimental setup and the alanine (with its holder) models, were validated by considering the same approach as used in Billas $et\,al\,(2020)$. Using a technique developed in that study, the effect of the air gaps, associated with the structure of the alanine pellets and the possible asymmetry of their positions inside the holder and for parallel orientation, in the two MRI-linac environments, were investigated. The results were used as the basis for estimating one component in the measurement uncertainty, which was found to be 0.55% and 0.17% for the Elekta UnityTM and the ViewRay MRIdian beam qualities, respectively.

The alanine magnetic field correction factor was obtained by dividing the product of the ratio of the absorbed dose to water with and without magnetic field and the ratio of the absorbed dose to alanine without and with a magnetic field, with the alanine relative intrinsic sensitivity, which was defined by Billas $et\ al\ (2020)$. The magnetic field strength and the beam energy of each MRI-linac system were considered. The $k_{Q_B,Q}^{al}$ values for the Elekta UnityTM and the ViewRay MRIdianTM were found to be $0.9957\ \pm\ 0.0059$ and $0.9997\ \pm\ 0.0028$, respectively.

4.2. Measurements and influence quantities on the detectors' signals

The measurement repeatability at each MRI-linac centre was found to be 0.1%, based on the variation from the readings (signal per MU) of an individual chamber, which was used repeatedly during the calibration of the secondary chambers at each centre. This includes the variation in the linac beam output, which was found to be very stable for both MRI-linac systems during the measurements. The linac-to-linac variation, on the Elekta UnityTM, may be reflected in the variation in the $TPR_{20,10}$ measurements. This was found to be 0.003 and 0.002 when the magnet was either on or off, respectively.

The effect of the magnetic field on the chamber signal depends on the chamber orientation and is smaller for the parallel orientation. The change in signal might be expected to lead to a proportional change in the volume recombination: measurements show that any change in ion recombination is small, and also subject to intrative variation.

On average, the $TPR_{20,10}$ value in the presence of a magnetic field was found to differ by 0.003 from the value at zero magnetic field, for both MRI-linac systems. This difference is within the variation of the measured $TPR_{20,10}$ at different Elekta UnityTM machines. We did not have enough data to make a similar conclusion for the ViewRay MRIdianTM machine, but, a change of 0.003 in the $TPR_{20,10}$ at 0 T, would result in a change in the chamber magnetic field correction factor of only 0.03% (on average), determined indirectly. This has been included in the uncertainty budget.

		$k_{Q_B,Q}$						
Chamber type	Study	<u></u>	↑↓	1				
PTW 30013	van Asselen <i>et al</i> (2018)		0.9920 ± 0.0020	0.9630 ± 0.0020				
	de Prez et al (2019b)		0.9850 ± 0.0060	0.9630 ± 0.0040				
	This study indirect	0.9926 ± 0.0038	0.9913 ± 0.0030	0.9612 ± 0.0027				
	This study direct	0.9954 ± 0.0050	0.9942 ± 0.0046	0.9626 ± 0.0030				
IBA FC65-G	van Asselen et al (2018)		0.9970 ± 0.0030	0.9520 ± 0.0020				
	de Prez et al (2019b)		0.9950 ± 0.0040	0.9560 ± 0.0040				
	This study indirect	0.9970 ± 0.0038	0.9963 ± 0.0027	0.9524 ± 0.0027				
	This study direct	1.0014 ± 0.0039	0.9994 ± 0.0056	0.9566 ± 0.0026				

The volume averaging correction factors, due to the non-uniform lateral beam profiles of the $10 \, \mathrm{cm} \times 10 \, \mathrm{cm}$ radiation field in the FFF beams of the Elekta UnityTM and the ViewRay MRIdianTM, were determined for the alanine and the Farmer-type chambers. The k_{vol} value of the ViewRay MRIdianTM, for both alanine and Farmer-type chamber, was found to be higher compared the Elekta UnityTM. This is because the lateral profile of the Elekta UnityTM is somewhat flatter, compared to the ViewRay MRIdianTM, which can be attributed to the difference in focal distance, partially offset by the difference in beam energy.

4.3. Farmer-type chamber calibration coefficients and validation of alanine as a transfer standard in zero magnetic field

The feasibility of using alanine as a reference class detector in the presence of magnetic fields has been demonstrated by Billas $et\,al\,(2020)$. The process of the absorbed dose to water measurements, followed in the current study, was validated at zero magnetic field. The dose measured with alanine was compared to the dose measured with a Farmer-type chamber at 0 T in an MRI-linac. On average, the ratio between the alanine-measured dose and the chamber-measured dose was found to be 0.9989 \pm 0.0006. This difference from unity, of -0.11%, is consistent with the combined standard uncertainty of the ratio, which is 0.62%. Note that the uncertainty of the ratio includes correlated contributions, such as the uncertainty of the NPL primary standard of absorbed dose to water. These correlated contributions cancel in the uncertainty of the ratio.

The present work successfully calibrated Farmer-type chambers (PTW 30013 and IBA FC65-G), by using alanine as a transfer standard, in an Elekta UnityTM and a ViewRay MRIdianTM systems when the constant magnetic field was switched off and on. A detailed explanation of the uncertainty budget is also provided. It was found that the overall combined standard uncertainty of the ionisation chamber calibration coefficient, N_{D,w,Q_B} , in the presence of a magnetic field, was 1.06% and 0.92% for the Elekta UnityTM and the ViewRay MRIdianTM, respectively.

The accuracy of the developed traceability route for reference dosimetry measurements and calibration of ionisation chambers in the presence of a magnetic field can be checked in a consistency test. The test was based on the variation of an ionisation chamber calibration coefficient, N_{D,w,Q_B} , for the different orientations, for different Elekta UnityTM systems. Variations were found (figure 9) of between 0.32% and 0.48% (average of 0.41%), which is within the standard uncertainty, even after the removal of correlated contributions, which reduces that standard uncertainty from 1.06% to 0.58%.

4.4. Farmer-type chamber magnetic field correction factors, $k_{Q_B,Q}$

The Farmer-type chamber magnetic field correction factors were determined for three different orientations of the chamber long axis with respect to the magnetic field and for both MRI-linac systems. Two different methods were applied: an indirect (section 2.3.1) and a direct (section 2.3.2). The absolute average difference between the $k_{Q_B,Q}$ values determined indirectly and directly (between all three orientations at both MRI-linac systems) was found to be 0.36%. Further comparison of the two methods of this study is presented in tables 5 and 6.

On average, the $k_{Q_B,Q}$ values in the anti-parallel orientation appears to be smaller compared with the values in the parallel orientation for both MRI-linac beam qualities (see results from this study in tables 5 and 6). However, the uncertainties are too large to allow a more precise conclusion on this small difference. On the other hand, the $k_{Q_B,Q}$ values for the perpendicular orientation are known (de Pooter *et al* 2021) to differ from the values for the parallel/anti-parallel orientations, for a field strength of 1.5 T, by up to 5%. In this work we found this difference, averaging overall chambers of each type, to be 3.4% (PTW 30013) and 4.7% (IBA FC65-G) for

Table 6. $k_{Q_{B},Q}$ values, determined from ViewRay MRIdian[™] machines, of the study from Krauss *et al* (2020) and of this study (indirect and direct methods) for the PTW 30013 and the IBA FC65-G Farmer-type chambers in parallel (↑↑), anti-parallel (↑↓) and perpendicular (⊥) orientations. The quoted uncertainties are standard uncertainties (k = 1).

				$k_{Q_B,Q}$	
Chamber type	Study	Centre/chamber sn	<u></u>	$\uparrow\downarrow$	
PTW 30013	Krauss et al (2020)	_	0.9936 ± 0.0078	_	0.9706 ± 0.0076
	This study indirect	IPC/3981	0.9993 ± 0.0072	0.9992 ± 0.0072	0.9724 ± 0.0070
		IPC/9923	1.0009 ± 0.0072	1.0002 ± 0.0072	0.9764 ± 0.0070
		GCUK/9923	0.9951 ± 0.0072	0.9939 ± 0.0072	0.9718 ± 0.0070
	This study direct	IPC/3981	0.9965 ± 0.0034	0.9963 ± 0.0034	0.9696 ± 0.0033
		IPC/9923	0.9976 ± 0.0034	0.9969 ± 0.0034	0.9732 ± 0.0033
IBA FC65-G	Krauss et al (2020)	_	0.9936 ± 0.0078	_	0.9668 ± 0.0075
	This study indirect	IPC/3520	0.9977 ± 0.0072	0.9994 ± 0.0072	0.9710 ± 0.0070
	This study direct	IPC/3520	0.9914 ± 0.0034	0.9931 ± 0.0034	0.9650 ± 0.0033

the Elekta Unity[™]. From our measurements in the ViewRay MRIdian[™] this difference decreases to 2.6% (PTW 30013) and 2.8% (IBA FC65-G).

4.5. Comparison of $k_{Q_B,Q}$ with results from other studies

The indirect and the direct determination of $k_{Q_B,Q}$ values of the Farmer-type chambers of this study are compared with values found in the literature (van Asselen *et al* 2018, de Prez *et al* 2019b, Krauss *et al* 2020). Only studies that have performed measurements in MRI-linac systems are considered for comparison in this work. The review by de Pooter *et al* (2021) points out that early publications on the determination of the $k_{Q_B,Q}$ did not consider fully the potential difficulties of dosimetry in magnetic fields. As a result, the uncertainty of those determinations is underestimated and, for this reason, in comparing results reported here with previous results, some studies have been excluded. We have excluded from our comparison studies where:

- (a) $k_{Q_B,Q}$ is determined in a non-MRI-linac environment, so that an MRI-linac beam quality cannot be achieved (and quality-dependent aspects of the magnetic field correction factor, including the effect of the magnetic field on the absorbed dose to water in homogeneous water, would increase the uncertainty),
- (b) the effective collection volume, in MC calculations of $k_{Q_B,Q}$, is not considered (such $k_{Q_B,Q}$ values may lead to errors of up to 1.4% (Pojtinger *et al* 2019), on Farmer-type chambers) and
- (c) $k_{Q_B,Q}$ is expressed as a ratio of chamber readings only, ignoring the effect of the magnetic field on absorbed dose to water in homogeneous water.

Tables 5 and 6 present the $k_{Q_B,Q}$ values determined from Elekta Unity[™] and ViewRay MRIdian[™] machines, respectively. Results from this study (indirect and direct methods) are compared with results from de Prez *et al* (2019b) and van Asselen *et al* (2018) (table 5) and from Krauss *et al* (2020) (table 6), for the PTW 30013 and IBA FC65-G Farmer-type chamber in parallel, anti-parallel and perpendicular orientations. Any difference between the $k_{Q_B,Q}$ values of the present work and the three studies, is consistent within the standard uncertainties. Notes:

- i. The parallel orientation in van Asselen $et\,al\,(2018)$ has the same orientation as the anti-parallel in the present and the de Prez $et\,al\,(2019\mathrm{b})$ work.
- ii. The $k_{Q_B,Q}$ values from the present study in table 5, are the average over the values obtained at different Elekta UnityTM machines, for each chamber type, orientation and method. Standard uncertainties reflect the variation between the $k_{Q_B,Q}$ values.
- iii. In table 6, the determination of $k_{Q_B,Q}$ in the study of Krauss *et al* (2020), involves a beam quality correction factor, k_{Q,Q_0} , taken from Andreo *et al* (2020). The standard uncertainty on their $k_{Q_B,Q}$ values results in 0.78%, which is the combination of the standard uncertainties on k_{Q,Q_0} (0.62%) and their results (0.48%). In the present study, the standard uncertainties have been estimated to be 0.72% and 0.34% for the indirect and the direct method, respectively.

5. Conclusion

This study established an alternative, robust and practical traceable reference dosimetry for, and calibration of, MRIgRT machines. An alanine dosimeter, calibrated with the NPL's primary standard in a conventional linac and corrected for the effect of magnetic fields, is used as a transfer standard for reference dosimetry measurements and calibration of secondary detectors. This traceability route may be applied to calibrate ionisation chambers in Elekta Unity™ and ViewRay MRIdian™ systems with a standard uncertainty of 1.1% and 0.9%, respectively. This study also reports values of magnetic field correction factors for Farmer-type chambers (PTW 30013 and IBA FC65-G), at three different orientations with respect to the magnetic field and for two different MRI-linac systems (Elekta Unity™ and the ViewRay MRIdian™). These values should be considered for inclusion in new data sets of correction factors for the development of the future protocols for reference dosimetry in MRIgRT.

Acknowledgments

The authors wish to thank Thijs Perik and Jochem Kaas from Netherlands Cancer Institute, Simeon Nill and Ian Hanson from the The Royal Marsden Hospital and The Institute of Cancer Research, Geoff Budgell, Joe Berresford and James Agnew from The Christie NHS Foundation Trust, Carsten Brink, Hans L Riis and Anders S Bertelsen from Odense University Hospital, Fau Pierre and Hugues Mailleux from Institute Paoli Calmettes, Marseille and Niall McAndrew and Ben George from GenesisCare, Oxford for access into their MRI-linac machines. They would also like to gratefully acknowledge Michael Homer, David Maughan and David Shipley from The National Physical Laboratory for assisting with measurements and MC simulations. The work was supported by the UK government's Department for Business, Energy and Industrial Strategy and the EMPIR programme, grant 15HLT08 and grant 19NRM01, co-financed by the Participating States and from the European Union's Horizon 2020 research and innovation programme. Research at The Institute of Cancer Research is supported by Cancer Research UK under Programme C33589/A28284 and NHS funding to the NIHR Biomedical Research Centre at The Royal Marsden Hospital and The Institute of Cancer Research.

Appendix

Tables A1 and A2 show the indirect and the direct, respectively, $k_{Q_B,Q}$ values of the PTW 30013 and the IBA FC65-G Farmer-type chambers for all visited centres, for the Elekta UnityTM and the ViewRay MRIdianTM systems. Results are presented for the three orientations of the chamber with respect to a magnetic field: parallel ($\uparrow\uparrow$), anti-parallel ($\uparrow\downarrow$) and perpendicular (\bot).

I Billas et al

Table A1. Indirect determination of the $k_{Q_B,Q}$ values of the PTW 30013 and the IBA FC65-G Farmer-type chambers for all visited centres, for both the Elekta Unity[™] and the ViewRay MRIdian[™] systems, with uncertainties for each value of 0.88% and 0.71%, respectively. Results are presented for the three orientations of the chamber with respect to a magnetic field (↑↑, ↑↓, ⊥).

						Elekta Unity™						
	11				↑↓					Т		
Chamber	Christie	ristie Odense	Odense	Christie	NKI	RMH/ICR	Christie	Odense	Christie	Christie	Odense	Christie
(type/sn)	(Sep 17)	(Jun 18)	(Mar 19)	(Dec 16)	(Mar 17)	(Sep 17)	(Jun 18)	(Mar 19)	(Sept 17)	(Jun 18)	(Mar 19)	
PTW 30013/3981	0.9963	0.9881	0.9891	0.9933	0.9885	0.9963	0.9892	0.9889	0.9641	0.9559	0.9584	
PTW 30013/9145					0.9854	0.9897						
PTW 30013/9486	0.9959		0.9906			0.9956		0.9905			0.9620	
PTW 30013/9487	1.0008		0.9911			0.9959		0.9906			0.9610	
PTW 30013/9923		0.9916					0.9920			0.9607		
PTW 30013/2181		0.9931					0.9911			0.9620		
PTW 30013/6157		0.9899					0.9916			0.9624		
PTW 30013/6158		0.9917					0.9916			0.9637		
IBA FC65-G/3520	1.0034	0.9972	0.9939	0.9946	0.9945	1.0019	0.9973	0.9948	0.9570	0.9512	0.9513	
IBA FC65-G/3821		0.9955	0.9950				0.9960	0.9950		0.9514	0.9513	
					ViewRay M	RIdian™						
		$\uparrow \uparrow$				$\uparrow\downarrow$				Т		
Chamber (type/sn)	IPC (May 19)		GCUK (Dec 19)		IPC (May 19)		GCUK (Dec 19)		IPC (May 19)		GCUK (Dec 19)	
PTW 30013/3981 PTW 30013/9923 IBA FC65-G/3520	0.9993 1.0009 0.9977		0.9951		0.9992 1.0002 0.9994		0.9939		0.9724 0.9764 0.9710		0.9718	

Table A2. Direct determination of the $k_{Q_B,Q}$ values of the PTW 30013 and the IBA FC65-G Farmer-type chambers for all visited centres, for both the Elekta Unity[™] and the ViewRay MRIdian[™] systems, with uncertainties for each value of 0.62% and 0.34%, respectively. Results are presented for the three orientations of the chamber with respect to a magnetic field (↑↑, ↑↓, ⊥).

						Elekta Unity™						
	11				11					Τ		
		Christie	Odense	Christie	RMH/ICR	Christie	Odense	Christie	RMH/ICR	Christie	Odense	Christie
Chamber (type/sn)	(Sep 17)	(Jun 18)	(Mar 19)	(Mar 17)	(Sep 17)	(Jun 18)	(Mar 19)	(Mar 17)	(Sep 17)	(Jun 18)	(Mar 19)	
PTW 30013/3981	0.9988	0.9937	0.9919	0.9878	0.9988	0.9948	0.9916	0.9878	0.9665	0.9614	0.9611	
PTW 30013/9145				0.9892				0.9892				
PTW 30013/9486	0.9953		0.9903		0.9950		0.9902				0.9617	
PTW 30013/9487	1.0067		0.9972		1.0017		0.9967				0.9669	
PTW 30013/9923		0.9952				0.9956				0.9642		
PTW 30013/2181		0.9939				0.9919				0.9628		
PTW 30013/3213		1.0015				1.0029				0.9557		
PTW 30013/6157		0.9908				0.9925				0.9633		
PTW 30013/6158		0.9900				0.9898				0.9620		
IBA FC65-G/3520	1.0073	1.0031	0.9981	0.9896	1.0059	1.0031	0.9990	0.9896	0.9608	0.9567	0.9553	
IBA FC65-G/3821		0.9999	0.9984			1.0005	0.9985			0.9557	0.9546	
					ViewRay MI	RIdian™						
		$\uparrow \uparrow$				$\uparrow\downarrow$						
Chamber (type/sn)	IPC (May 19)			IPC (May 19)			IPC (May 19)					
PTW 30013/3981		0.9965				0.9963				0.9696		
PTW 30013/9923		0.9976				0.9969				0.9732		
IBA FC65-G/3520		0.9914				0.9931				0.9650		

ORCID iDs

Ilias Billas https://orcid.org/0000-0002-0446-1723

References

Acharya S et al 2016 Online magnetic resonance image guided adaptive radiation therapy: first clinical applications Int. J. Radiat. Oncol. Biol. Phys. 94 394–403

Agnew J, O'Grady F, Young R, Duane S and Budgell G J 2017 Quantification of static magnetic field effects on radiotherapy ionization chambers *Phys. Med. Biol.* 62 1731–43

Almond PR, Biggs PJ, Coursey BM, Hanson WF, Huq MS, Nath R and Rogers DW O 1999 AAPM's TG-51 protocol for clinical reference dosimetry of high-energy photon and electron beams *Med. Phys.* 26 1847–70

Andreo P, Burns DT, Hohlfeld K, Huq MS, Kanai T, Laitano F, Smyth V and Vynckier S 2000 Absorbed dose determination in external beam radiotherapy: an international code of practice for dosimetry based on standards of absorbed dose to water *Technical Reports* Series no. 398 (Austria: International Atomic Energy Agency, Vienna)

Andreo P et al 2020 Determination of consensus k Q values for megavoltage photon beams for the update of IAEA TRS-398 Phys. Med. Biol. 65 095011

Anton M, Kapsch R P, Krauss A, von Voigts-Rhetz P, Zink K and McEwen M 2013 Difference in the relative response of the alanine dosimeter to megavoltage x-ray and electron beams *Phys. Med. Biol.* 58 3259–82

Bergstrand E S, Bjerke H and Hole E O 2005 An experimental investigation of the electron energy dependence of the EPR alanine dosimetry system Radiat. Meas. 39 21–8

Bergstrand E S, Shortt K R, Ross C K and Hole E O 2003 An investigation of the photon energy dependence of the EPR alanine dosimetry system *Phys. Med. Biol.* 48 1753–71

Billas I, Bouchard H, Oelfke U and Duane S 2019 The effect of magnetic field strength on the response of Gafchromic EBT-3 film *Phys. Med. Biol.* 64 06NT03

Billas I, Bouchard H, Oelfke U, Shipley D R, Gouldstone C A and Duane S 2020 Alanine dosimetry in strong magnetic fields: use as a transfer standard in MRI-guided radiotherapy *Phys. Med. Biol.* 65 115001

Billas I, Maughan D, Costa F, Perik T, Kaas J and Duane S 2017 Determination of the magnetic field correction factor for ionisation chambers in an MR-Linac using alanine dosimetry 5th MR in RT Symp. (Sydney, Australia)

Boag J W and Current J 1980 Current collection and ionic recombination in small cylindrical ionization chambers exposed to pulsed radiation Br. J. Radiol. 53471-8

Cervantes Y, Billas I, Shipley D R, Duane S and Bouchard H 2020 Small-cavity chamber dose response in megavoltage photon beams coupled to magnetic fields *Phys. Med. Biol.* 65 245008

Costa F, Doran S J, Hanson I M, Nill S, Billas I, Shipley D, Duane S, Adamovics J and Oelfke U 2018 Investigating the effect of a magnetic field on dose distributions at phantom-air interfaces using PRESAGE (R) 3D dosimeter and Monte Carlo simulations *Phys. Med. Biol.* 63

D'Souza M, Nusrat H, Iakovenko V, Keller B, Sahgal A, Renaud J and Sarfehnia A 2020 Water calorimetry in MR-linac: Direct measurement of absorbed dose and determination of chamber *Med. Phys.* 47 6458–69

de Pooter J, Billas I, de Prez L, Duane S, Kapsch R-P, Karger C P, van Asselen B and Wolthaus J 2021 Reference dosimetry in MRI-linacs: evaluation of available protocols and data to establish a code of practice *Phys. Med. Biol.* 66 05TR02

de Prez L, de Pooter J, Jansen B, Wolthaus J, van Asselen B, Woodings S, Soest T, Kok J and Raaymakers B 2016 First water calorimetric dw measurement and direct measurement of magnetic field correction factors, KQ, B, in a 1.5 T B-field of an MRI linac *Med. Phys.*43 3874

de Prez L, de Pooter J, Jansen B, Woodings S, Wolthaus J, van Asselen B, van Soest T, Kok J and Raaymakers B 2019a Commissioning of a water calorimeter as a primary standard for absorbed dose to water in magnetic fields *Phys. Med. Biol.* 64 035013

de Prez L, Woodings S, de Pooter J, van Asselen B, Wolthaus J, Jansen B and Raaymakers B 2019b Direct measurement of ion chamber correction factors, k(Q) and k(B), in a 7 MV MRI-linac *Phys. Med. Biol.* 64 105025

Delfs B, Schoenfeld A A, Popping D, Kapsch R P, Jiang P, Harder D, Poppe B and Looe H K 2018 Magnetic fields are causing small, but significant changes of the radiochromic EBT3 film response to 6 MV photons *Phys. Med. Biol.* 63 035028

Eaton D J, Bass G, Booker P, Byrne J, Duane S, Frame J, Grattan M, Thomas R A S, Thorp N and Nisbet A 2020 IPEM code of practice for high-energy photon therapy dosimetry based on the NPL absorbed dose calibration service *Phys. Med. Biol.* 65 195006

Fischer-Valuck B W et al 2017 Two-and-a-half-year clinical experience with the world's first magnetic resonance image guided radiation therapy system Adv. Radiat. Oncol. 2 485–93

Hackett S L, van Asselen B, Wolthaus J W H, Kok J G M, Woodings S J, Lagendijk J J W and Raaymakers B W 2016 Consequences of air around an ionization chamber: are existing solid phantoms suitable for reference dosimetry on an MR-linac? *Med. Phys.* 43 3961–8

Joint Committee for Guides in Metrology 2008 Evaluation of measurement data—Guide to the expression of uncertainty in measurement. JCGM 100:2008 (Paris: International Bureau of Weights and Measures (BIPM)) (GUM 1995 with minor corrections)

Kawrakow I 2000 Accurate condensed history Monte Carlo simulation of electron transport: II. Application to ion chamber response simulations Med. Phys. 27 499–513

Kawrakow I, Mainegra-Hing E, Rogers D W O, Tessier F and Walters B R 2011 The EGSnrc Code System: Monte Carlo Simulation of Electron and Photon Transport NRCC Report PIRS-701 (Ottawa: National Research Council of Canada)

Kluter S 2019 Technical design and concept of a 0.35 T MR-Linac Clin. Transl. Radiat. Oncol. 18 98–101

Krauss A, Spindeldreier C K and Klüter S 2020 Direct determination of k B, Q, Q0 for cylindrical ionization chambers in a 6 MV 0.35 T MR-linac *Phys. Med. Biol.* 65 235049

Lillicrap S C, Owen B, Williams J R and Williams P C 1990 Code of practice for high-energy photon therapy dosimetry based on the NPL absorbed dose calibration service *Phys. Med. Biol.* 35 1355–60

Malkov V and Rogers D 2016 Charged particle transport in magnetic fields in EGSnrc Med. Phys. 43 4447–58

Malkov V N and Rogers D W O 2017 Sensitive volume effects on Monte Carlo calculated ion chamber response in magnetic fields *Med. Phys.*44 4854–8

Malkov V N and Rogers D W O 2019 Monte Carlo study of ionization chamber magnetic field correction factors as a function of angle and beam quality (vol 45, pg 908, 2018) *Med. Phys.* 46 5367–70

- Mutic S and Dempsey J F 2014 The ViewRay System: magnetic resonance-guided and controlled radiotherapy Semin. Radiat. Oncol. 24 196–9
- O'Brien D J, Roberts D A, Ibbott G S and Sawakuchi G O 2016 Reference dosimetry in magnetic fields: formalism and ionization chamber correction factors *Med. Phys.* 43 4915–27
- Palmans H, Andreo P, Huq S, Seuntjens J, Christaki K and Meghzifene A 2017 Dosimetry of Small Static Fields Used in External Beam Radiotherapy (Vienna: International Atomic Energy Agency)
- Pojtinger S, Dohm O S, Kapsch R P and Thorwarth D 2018 Ionization chamber correction factors for MR-linacs *Phys. Med. Biol.* 63 11NT03 Pojtinger S, Kapsch R P, Dohm O S and Thorwarth D 2019 A finite element method for the determination of the relative response of ionization chambers in MR-linacs: simulation and experimental validation up to 1.5 T *Phys. Med. Biol.* 64 135011
- Raaymakers B W et al 2017 First patients treated with a 1.5 T MRI-Linac: clinical proof of concept of a high-precision, high-field MRI guided radiotherapy treatment Phys. Med. Biol. 62 L41–50
- Raaymakers B W, Raaijmakers A J E, Kotte A, Jette D and Lagendijk J J W 2004 Integrating a MRI scanner with a 6 MV radiotherapy accelerator: dose deposition in a transverse magnetic field *Phys. Med. Biol.* 49 4109–18
- Reynolds M, Fallone B G and Rathee S 2013 Dose response of selected ion chambers in applied homogeneous transverse and longitudinal magnetic fields *Med. Phys.* 40 042102-7
- Sharpe P H G 2003 Report on Radiation Dosimetry at NPL CCRI(I)/03-14 (Paris: International Bureau of Weights and Measures (BIPM))
 Spindeldreier C K, Schrenk O, Bakenecker A, Kawrakow I, Burigo L, Karger C P, Greilich S and Pfaffenberger A 2017 Radiation dosimetry in magnetic fields with farmer-type ionization chambers: determination of magnetic field correction factors for different magnetic field strengths and field orientations Phys. Med. Biol. 62 6708–28
- Thomas S J, Aspradakis M M, Byrne J P, Chalmers G, Duane S, Rogers J, Thomas R A S, Tudor G S J, Twyman N and Party I W 2014 Reference dosimetry on tomotherapy: an addendum to the 1990 UK MV dosimetry code of practice *Phys. Med. Biol.* 59 1339–52
- Trachsel M A, Pojtinger S, Meier M, Schrader M, Kapsch R-P and Kottler C 2020 Chemical radiation dosimetry in magnetic fields: characterization of a fricke-type chemical detector in 6 MV photon beams and magnetic fields up to 1.42 T *Phys. Med. Biol.* 65 065005
- van Asselen B, Woodings S J, Hackett S L, van Soest T L, Kok J G M, Raaymakers B W and Wolthaus J W H 2018 A formalism for reference dosimetry in photon beams in the presence of a magnetic field *Phys. Med. Biol.* 63 125008
- Zeng G G, McEwen M R, Rogers D W O and Klassen N V 2004 An experimental and Monte Carlo investigation of the energy dependence of alanine/EPR dosimetry: I. Clinical x-ray beams *Phys. Med. Biol.* 49 257–70